Semiclassical limitations for photon emission in strong external fields

E. Raicher,[1,*] S. Eliezer,[2,3] C. H. Keitel,[1] and K. Z. Hatsagortsyan[1,†]
[1]*Max-Planck-Institut für Kernphysik, Saupfercheckweg 1, 69117 Heidelberg, Germany*
[2]*Department of Applied Physics, Soreq Nuclear Research Center, Yavne 81800, Israel*
[3]*Nuclear Fusion Institute, Polytechnic University of Madrid, Madrid, Spain*

(Received 15 October 2018; published 28 May 2019)

The semiclassical heuristic radiation formula of Baier and Katkov [V. N. Baier and V. M. Katkov, Sov. Phys. JETP **26**, 854 (1968)] is well known to describe radiation of an ultrarelativistic electron in strong external fields employing the electron classical trajectory. To find the limitations of the Baier-Katkov approach, we investigate an electron radiation in a strong rotating electric field quantum mechanically using the Wentzel-Kramers-Brillouin approximation. It is shown that an additional condition except for an ultrarelativistic velocity is required in order to recover this widely used result. A violation of this condition gives rise to a qualitative discrepancy in the harmonic spectra between the two approaches. Furthermore, the same classical trajectory in the rotating electric field and in a plane-wave field is shown to produce substantially different spectra, in contradiction to the semiclassical paradigm. In particular, the number of absorbed field photons, and thus the amount of energy absorbed from the field during emission, are different in these cases.

DOI: 10.1103/PhysRevA.99.052513

I. INTRODUCTION

In recent years, the achievable intensities of both optical [1–3] and x-ray [4,5] lasers have been rapidly rising and a plethora of unexplored physical phenomena are expected to come within reach [6–14]. The fundamental theory describing these phenomena is strong-field QED, which concerns the dynamics of quantum relativistic particles in the presence of strong electromagnetic (EM) fields. The strong-field regime is characterized by a considerable nonlinearity parameter $\xi \gtrsim 1$ [15], with $\xi \equiv ea/m = 7.5\sqrt{I_L/(10^{20}\ \mathrm{W/cm^2})}/\omega[(\mathrm{eV})]$, where $-e$ and m are the electron charge and mass, respectively, a is the amplitude of the laser vector potential A_μ, and I_L, ω are the laser intensity and frequency, respectively. Relativistic units $\hbar = c = 1$ are used throughout.

In the realm of the Furry picture, which is commonly employed in strong-field QED, the strong EM field is considered as a classical field and is included in the free part of the Lagrangian [16]. As a consequence, the free particles in the standard QED perturbation theory are replaced with particles experiencing the external field. Especially successful is this formalism for field configurations which admit an exact analytical solution for the electron wave function: plane-wave field (PWF) [17], static electric field [18], static magnetic field [19,20], and PWF combined with a static magnetic field [21]. The rates of the scattering processes of electrons, positrons, and photons in the presence of a laser field calculated in this framework [15,22–33] depend upon ξ, as well as on the quantum parameter $\chi \equiv e\sqrt{-(F^{\mu\nu}P_\nu)^2}/m^3$, where $P_\nu = (\mathcal{E}, \mathbf{P})$ is the kinetic four-momentum and $F_{\mu\nu} = \partial_\mu A_\nu - \partial_\nu A_\mu$ the field tensor. A bold letter designates a three vector. Of special interest are the lowest-order processes, namely, the nonlinear Compton, $e^- + n\gamma_F \to e^- + \gamma$, and nonlinear Breit-Wheeler scatterings, $\gamma + n\gamma_F \to e^- + e^+$ (where $e^+, e^-, \gamma, \gamma_F$ represent a positron, an electron, a gamma photon, and a photon associated with the external field, respectively). They differ from the standard Compton and Breit-Wheeler processes by the fact that they involve many incoming photons interacting coherently with the fermions. These processes may lead to an avalanchelike phenomenon ("QED cascade"), where an electron emits a gamma photon, which interacts with the laser field to produce an electron-positron pair, and so on, resulting in the rapid formation of copious electron-positron pairs plasma [34–38].

Laser plasma experiments are expected to involve complex field configurations, as opposed to the simplified nature of the analytical solutions mentioned above. A possible way to overcome this obstacle is to rely on the semiclassical (SC) method, introduced by Baier and Katkov [39,40]. It allows one to calculate the emission rate, including photon recoil effects, in a general field configuration, given that the particle motion is quasiclassical and ultrarelativistic. This method does not require the particle wave function, but only its classical trajectory in the given field configuration. In the ultrastrong-field regime ($\xi \gg 1$), a simpler approach is being commonly applied. It employs the local constant field approximation (LCFA), formulated by Nikishov and Ritus [23] in the 1960s. They argued that as long as

$$\mathcal{F}, \mathcal{G} \ll \chi^2, \quad \mathcal{F}, \mathcal{G} \ll 1, \quad \xi \gg 1 \tag{1}$$

are satisfied, a particle emits radiation as if it was immersed in a constant crossed field. The quantities $\mathcal{F} \equiv e^2 F_{\mu\nu}F^{\mu\nu}/(4m^4)$ and $\mathcal{G} \equiv \epsilon_{\alpha\beta\mu\nu}e^2F^{\alpha\beta}F^{\mu\nu}/(4m^4)$ are the field invariants and the symbol $\epsilon_{\alpha\beta\mu\nu}$ stands for the Levi-Civita tensor. Following this assumption, the radiative processes are described by analytical expressions regardless of the exact temporal

*erez.raicher@mpi-hd.mpg.de
†karen.hatsagortsyan@mpi-hd.mpg.de

and spatial shape of the EM field. This attitude underlies the QED emission modules [41–43] integrated in particle-in-cell plasma simulations (see, also, improved versions of the LCFA expression [44–46]). Recently, an approximated wave function describing an ultrarelativistic electron interacting with a tightly focused laser beam was proposed [47] and employed for calculating the rates of QED processes in such fields [48–50]. Given the increasingly extreme and complex scenarios being explored with further rising laser intensities and frequencies, there is an urgent need to benchmark and investigate the limitations of the SC and LCFA approximations.

A relatively simple but not exactly solvable field configuration is the rotating electric field (REF). Its physical significance stems from the fact that it describes a particle in a plasma wave (in a frame that moves with the wave group velocity) or a particle in the antinode of a standing wave, created by two counterpropagating laser beams. The latter is one of the favorite configurations to examine QED cascades [41–43]. In principle, the electron's motion in a standing wave is complex and is not limited to the antinodes. However, in the anomalous radiative trapping regime (corresponding to ξ values above several thousands), the electrons are expected to be trapped in the antinodes [51]. The wave function associated with this configuration has been excessively studied [52–57]. Recently, quantum calculations of the emitted radiation in this configuration have been carried out [58,59], using various approximations for the wave function.

In the present paper, the quantum radiation emitted by a particle in a REF is calculated using the Wentzel-Kramers-Brillouin (WKB) method, which is more accurate than the approaches employed so far for this scenario. The full quantum calculation of the radiation spectra is used as a benchmark for the SC approach. We demonstrate that a further condition is required except for an ultrarelativistic motion: the γ factor of the particle ($\gamma = \mathcal{E}/m \gg 1$) should be much larger than the nonlinearity parameter ξ. As a test case, a particle moving in a circle in REF is studied. For this case, the condition $\gamma \gg \xi$ is violated and, therefore, the WKB and SC approaches yield different emission spectra. According to both models, the spectrum takes the form of discrete harmonics, but with qualitatively different harmonic structure (although, with the same harmonic-averaged spectrum). As the circlelike electron's trajectory is also possible for a particle counterpropagating a PWF laser with a certain initial momentum, we compare our emission spectrum to the latter case as well. For the PWF (at $\xi \gg 1$), a continuous spectrum, coinciding with the LCFA result, is predicted, in contrast to the discrete spectrum in REF. Moreover, for the REF case, a cutoff in the number of absorbed photons is predicted, while the PWF does not exhibit such a restriction. It implies that the depletion of the field energy should be essentially different. Furthermore, the observed discrepancy indicates that the emission spectrum in the quantum recoil regime cannot be fully determined by the electron's classical trajectory. Namely, the particular EM field driving the motion should be taken into consideration as well. Additionally, the REF result demonstrates that the exact spectrum may deviate from the LCFA result even though the Ritus-Nikishov condition of Eq. (1) is satisfied. Rather, the coincidence with the LCFA is achieved for the harmonic-averaged spectrum only.

The paper is organized as follows. In Sec. II A, the emission expression is derived quantum mechanically using the WKB wave function. Section II B summarizes the SC approach. The quantum and semiclassical results are compared in Sec. III, and the applicability condition of the SC formula is deduced. Section IV deals with a specific case—circular motion—and contains the corresponding harmonics energy as well as matrix element calculations according to both models. In Sec. V, the numerical results are presented and the physical consequences of our findings are discussed and concluded in Sec VI.

II. PHOTON EMISSION EXPRESSION

A. WKB approach

In the following, the radiation emitted by an electron in a REF is calculated using the WKB approximation for the wave function. For the sake of simplicity, the spin effect is neglected, which is justified as long as $\chi \lesssim 1$ [15]. Thus the electron wave function in a strong electromagnetic field is described by the Klein-Gordon equation:

$$[-\hbar^2\partial^2 - 2ie\hbar(A\cdot\partial) + e^2A^2 - m^2]\Phi = 0, \tag{2}$$

where the reduced Planck constant $\hbar$ is explicitly written, as it plays a key role in the WKB approximation. The vector potential corresponding to REF is given by

$$A^\mu = a_1^\mu \cos(k\cdot x) + a_2^\mu \sin(k\cdot x), \tag{3}$$

where $a_1^\mu = a(0,1,0,0)$, $a_2^\mu = a(0,0,1,0)$ are the polarization vectors, $k = (\omega,0,0,0)$ is the wave vector in the laboratory frame, and ω is the field frequency. The vector potential (and therefore the electric field as well) is assumed to vanish for asymptotic times ($t \to \pm\infty$) and to be turned on adiabatically, so that its time and space derivatives can be neglected. Notice that $k^2 \neq 0$, in contrast to the PWF case. Hence, Eq. (2) cannot be reduced to a first-order equation. In the following, the leading-order WKB approximation is employed [60,61]. Namely, we seek for a solution of the form

$$\Phi = \exp\left[\left(\frac{S_0}{\hbar} + S_1\right)\right]. \tag{4}$$

By substituting Eq. (4) into Eq. (2), neglecting the second-order terms in $\hbar$, and equating the coefficients of each $\hbar$ power to zero, one finds

$$S_0 = i\left(\int_{-\infty}^{t} dt'\mathcal{E}(t') - \mathbf{p}\cdot\mathbf{x}\right), \quad S_1 = -\frac{1}{2}\ln\mathcal{E}(t), \tag{5}$$

where p_μ is the initial momentum (i.e., the momentum prior to the field switching on) and S_0 is the classical action, as expected. The kinetic momentum and energy are given by

$$\mathcal{E}(t) = \sqrt{m^2 + \mathbf{P}^2(t)}, \quad \mathbf{P}(t) = \mathbf{p} - e\mathbf{A}(t). \tag{6}$$

For the sake of simplicity, the explicit time dependence of $\mathcal{E}$, $\mathbf{P}$ will be discarded from now on. Accordingly, the approximated wave function reads

$$\Phi_p = \frac{1}{\sqrt{2V\mathcal{E}}}\exp\left[i\left(\int_{-\infty}^{t} dt'\mathcal{E} - \mathbf{p}\cdot\mathbf{x}\right)\right], \tag{7}$$

where V is the normalization volume and the $\hbar$ will be omitted henceforth. Notice that for a general EM field configuration,

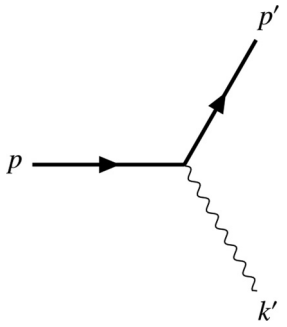

FIG. 1. The Feynmann diagram representing the emission process. The bold lines represent the "dressed" electron in the Furry picture.

the classical action and trajectory cannot be found analytically and therefore the WKB is not beneficial. In our case, however, the classical motion admits an analytical solution.

The transition amplitude for the leading-order nonlinear photon emission, depicted as a Feynman diagram in Fig. 1, is given [58] by

$$iT = e\epsilon^{\mu}\int dx^4 \frac{e^{-ik'\cdot x}}{\sqrt{2\omega'}} \times [\Phi^*_{p'}(\partial_\mu + eA_\mu)\Phi_p - \Phi_{p'}(\partial_\mu - eA_\mu)\Phi^*_p], \quad (8)$$

where the $*$ symbol stands for a complex conjugate, ϵ is the emitted photon polarization vector, and p, p', k' are the momenta associated with the incoming electron, outgoing electron, and emitted photon, respectively. Substituting the wave function given by Eq. (4) leads to

$$iT = (2\pi)^3 e\epsilon^{\mu}\int_{-\infty}^{\infty} dt\left[\frac{P_\mu + P'_\mu}{\sqrt{8\omega'\mathcal{E}\mathcal{E}'}}\right]e^{i\psi}\delta^3(\mathbf{p}-\mathbf{p}'-\mathbf{k}'), \quad (9)$$

where the argument reads

$$\psi = \omega' t + \int_{\infty}^{t} dt'\mathcal{E}' - \int_{-\infty}^{t} dt'\mathcal{E}. \quad (10)$$

It follows from the δ function in Eq. (9) that the initial momenta of the incoming and outgoing particles are related through $\mathbf{p}' = \mathbf{p} - \mathbf{k}'$. Together with Eq. (6), it leads to

$$\mathcal{E}' = \sqrt{m^2 + \mathbf{P}'^2}, \quad \mathbf{P}' = \mathbf{P} - \mathbf{k}'. \quad (11)$$

Using the expression of Eq. (11) for $\mathbf{P}'$, and since the temporal component of ϵ_μ vanishes, we have

$$\epsilon\cdot[P + P'] = -\boldsymbol{\epsilon}\cdot[2\mathbf{P} - \mathbf{k}'] = 2\epsilon\cdot P, \quad (12)$$

where the orthogonality relation $\epsilon\cdot k' = 0$ was used. Finally, one obtains

$$iT = \frac{(2\pi)^3}{\sqrt{2}} e\mathcal{T}_{if}\delta^3(\mathbf{p}-\mathbf{p}'-\mathbf{k}'), \quad (13)$$

where

$$\mathcal{T}_{if} \equiv \int_{t_i}^{t_f} dt' \frac{[\epsilon\cdot P]}{\sqrt{\omega'\mathcal{E}\mathcal{E}'}} e^{i\psi}. \quad (14)$$

Due to the periodicity of the field, one may decompose the phase into

$$\psi = \psi_p + \psi_{np}\omega t, \quad \psi_{np} \equiv \frac{1}{T}\int_0^T \psi(t')dt', \quad (15)$$

where ψ_p and ψ_{np} are the periodic and nonperiodic parts, correspondingly, and $T = 2\pi/\omega$ is the EM field period. Consequently, Eq. (14) may be written as a series of δ functions,

$$\mathcal{T}_{if} = 2\pi\sum_s \mathcal{M}_s\delta(\Omega_s), \quad \Omega_s \equiv \omega(s - \psi_{np}). \quad (16)$$

The matrix element corresponding to a s-photon process is given by

$$\mathcal{M}_s \equiv \frac{1}{T}\int_0^T dt\left[\frac{\epsilon\cdot P}{\sqrt{\omega'\mathcal{E}\mathcal{E}'}}\right]e^{i\psi_p - s\omega t}. \quad (17)$$

Since according to the momentum conservation appearing in Eq. (13), $\mathbf{p}'$ is determined by $\mathbf{k}'$, it follows that Ω_s can be written as a function of $\mathbf{k}'$. Hence, the requirement $\Omega_s = 0$, corresponding to the energy conservation, imposes a restriction on the wave vector of the emitted photon. Writing ψ_{np} explicitly, one arrives at

$$\Omega_s = s\omega + \mathcal{E}_{av} - \omega' - \mathcal{E}'_{av} = 0, \quad (18)$$

where $\mathcal{E}_{av}$ and $\mathcal{E}'_{av}$ are the cycle-averaged value of $\mathcal{E}$ and $\mathcal{E}'$, respectively.

The emission probability $\mathcal{P}$ is obtained by integrating the squared transition amplitude over the phase space of the outgoing particle [62],

$$\mathcal{P} = \int \frac{Vd^3\mathbf{p}'}{(2\pi)^3}\frac{Vd^3\mathbf{k}'}{(2\pi)^3}|iT|^2. \quad (19)$$

The squared transition amplitude given by Eq. (13) takes the form

$$|iT|^2 = \frac{(2\pi)^3 e^2}{2}\delta^3(\mathbf{p}-\mathbf{p}'-\mathbf{k}')V|\mathcal{T}_{if}|^2. \quad (20)$$

One may see that the volume V is canceled with the normalization factor of the wave functions included in $\mathcal{T}_{if}$. Consequently, it will be omitted from now on. Plugging Eq. (20) into Eq. (19) and taking advantage of the spatial δ function, one arrives at

$$\mathcal{P} = \frac{\alpha}{(2\pi)^2}\int d^3\mathbf{k}'|\mathcal{T}_{if}|^2, \quad (21)$$

where $\alpha = e^2/(4\pi) \approx 1/137$ is the fine-structure constant. Squaring $\mathcal{T}_{if}$ yields

$$|\mathcal{T}_{if}|^2 = 2\pi\sum_{s,\epsilon}|\mathcal{M}_s|^2\delta(\Omega_s)\tau, \quad (22)$$

where τ is the interaction time which goes to infinity since we assume that the pulse is very long. Substituting Eq. (22) into Eq. (21), we obtain, for the rate (the probability per unit time $\mathcal{R} \equiv \lim_{\tau\to\infty}\frac{1}{\tau}\mathcal{P}$),

$$\mathcal{R} = \sum_s \mathcal{R}_s, \quad \mathcal{R}_s = \frac{\alpha}{2\pi}\int d^3\mathbf{k}'\sum_\epsilon |\mathcal{M}_s|^2\delta(\Omega_s). \quad (23)$$

Writing $d^3\mathbf{k}'$ explicitly in spherical coordinates and recalling the relation $dI = \omega' d\mathcal{R}$, we obtain, for the emitted intensity,

$$I_s = \frac{\alpha}{2\pi}\int d\omega' d(\cos\theta) d\varphi \omega'^3 \sum_{\epsilon} |\mathcal{M}_s|^2 \delta(\Omega_s), \tag{24}$$

where θ, φ are the polar and azimuthal emission angles, respectively.

B. SC approach

The SC operator technique, developed by Baier and Katkov [39,40], is a powerful method capable of calculating the emission radiated by a particle taking into account the recoil effect (corresponding to non-negligible χ). Its main virtue is that it applies for a general EM field and requires a solution of the classical rather than the quantum equation of motion. Its only limitations concern the nature of the particle dynamics. Namely, it should be ultrarelativistic and quasiclassical. For a free particle, the latter simply means that the particle oscillation frequency, induced by the EM field, is much lower as compared to the particle energy ($\omega \ll \mathcal{E}$). For a particle in a potential well, the quasiclassical regime is determined by the quantum index n associated with the bound levels. It was recently shown that for $n \gg 1$, the full quantum calculation for the emission coincides with the SC prediction [63,64].

The quasiclassical condition is required for the WKB approximation as well. Nevertheless, there are two reasons why the quantum calculation employing the WKB wave functions is superior to the Baier-Katkov SC model, thus making the benchmark significant. First, the SC approach relies on further assumptions beside the quasiclassical dynamics, such as the above-mentioned requirement $\gamma \gg 1$. Second, regarding the semiclassical assumption itself, in the Baier-Katkov derivation, it takes the form of neglecting certain commutation relations associated with the quantum operators. As these commutation relations can be calculated only for special cases (i.e., magnetic field), the justification for this neglect is questionable. Moreover, their formalism does not allow us to quantitatively evaluate its accuracy by considering high-order corrections. On the contrary, the WKB wave function is derived as an asymptotic series, taking the limit $\hbar \to 0$. As a result, a clear applicability criterion exists, deduced from the estimation of the neglected higher orders. In addition, one may, in principle, take further terms into account and thus evaluate the higher-orders correction to the wave function.

The emission probability for a scalar particle corresponding to this approach is given, analogously to Eq. (21),

$$\mathcal{P} = \frac{\alpha}{(2\pi)^2}\int d^3\mathbf{k}' |\widetilde{\mathcal{T}}_{if}|^2, \tag{25}$$

where the tilde symbol designates the SC approximation, and the following quantity is introduced [39,40]:

$$\widetilde{\mathcal{T}}_{if} \equiv \int_{t_i}^{t_f} dt' \left[\frac{\epsilon\cdot P}{\sqrt{\mathcal{E}(\mathcal{E}-\omega')\omega'}}\right] e^{i\widetilde{\psi}}. \tag{26}$$

The phase is given by

$$\widetilde{\psi} \equiv \left(\frac{\mathcal{E}}{\mathcal{E}-\omega'}\right)[k'\cdot x(t)], \tag{27}$$

where $x_\mu = [t, \mathbf{x}(t)]$ is the classical trajectory associated with the particle motion prior to the emission. The above expression for the emission probability contains a nontrivial statement. Namely, it argues that the classical trajectory solely determines the radiation, regardless of the driving EM field properties. This paradigm is challenged by the results appearing in Sec. V of this paper. The emission rate is given by Eq. (23), where Ω_s, $\mathcal{M}_s$ are replaced,

$$\widetilde{\mathcal{M}}_s = \frac{1}{T}\int_0^T dt \left[\frac{\epsilon\cdot P}{\sqrt{\mathcal{E}(\mathcal{E}-\omega')\omega'}}\right] e^{i\widetilde{\psi}_p - s\omega t}, \tag{28}$$

and

$$\widetilde{\Omega}_s \equiv \omega(s - \widetilde{\psi}_{np}), \tag{29}$$

respectively. The periodic and nonperiodic parts of the phase ($\widetilde{\psi}_p$, $\widetilde{\psi}_{np}$) are determined by averaging Eq. (27) on a single cycle, analogous to Eq. (15) with the modification $\psi \to \widetilde{\psi}$.

III. COMPARISON BETWEEN SC AND WKB

The aim of this section is to benchmark the SC result with the quantum calculation. In particular, we seek a validity criterion for the SC approach. Comparing Eqs. (14) and (26), it is clearly seen that the main discrepancy lies in the difference between ψ and $\widetilde{\psi}$. Since $\mathcal{E}'$ appears in Eq. (10) but not in Eq. (27), let us express it in terms of $\mathcal{E}$, ω'. Rewriting Eq. (11) in a more convenient way, we have

$$\mathcal{E}' = \sqrt{(\mathcal{E}-\omega')^2 - 2k'\cdot P}. \tag{30}$$

As SC generally requires $\mathcal{E}' \approx \mathcal{E} - \omega'$, one of the two key approximations required in order to recover SC is

$$\Xi_1 \equiv \frac{k'\cdot P}{(\mathcal{E}-\omega')^2} \ll 1. \tag{31}$$

As a result, one may Taylor expand $\mathcal{E}'(t)$. Substituting it in Eq. (10) for ψ, three terms cancel out and one obtains

$$\psi \approx \int_{-\infty}^{t} dt \left(\frac{\mathcal{E}}{\mathcal{E}-\omega'}\right)[k'\cdot v(t)], \tag{32}$$

where the four-momentum and energy are related by the four-velocity v_μ, $P_\mu = \mathcal{E}v_\mu$. In the Baier-Katkov approach, the factor $\mathcal{E}/(\mathcal{E}-\omega')$ is regarded as a constant in the time integration appearing in Eq. (32). The latter requires a further assumption that $\mathcal{E}$ should be approximately constant. Since, generally speaking, the energy $\mathcal{E}$ is oscillating in time, we formulate this condition as

$$\Xi_2 \equiv \frac{|\mathcal{E}-\mathcal{E}_{av}|}{\mathcal{E}_{av}} \ll 1, \tag{33}$$

where $|\mathcal{E}-\mathcal{E}_{av}|$ is the deviation of $\mathcal{E}$ from the cycle average value $\mathcal{E}_{av}$. Hence, for Ξ_1, $\Xi_2 \ll 1$, the WKB and SC expressions coincide.

Having obtained the mathematical requirements for the equivalence between the two approaches, let us discuss the physical conditions for which they are satisfied. First, notice that in the classical limit ($\omega' \ll \mathcal{E}$), Eqs. (31) and (33) are both satisfied and the classical emission formula is recovered. From now on, the quantum case is considered, namely, ω' is smaller than $\mathcal{E}$ but of the same order of magnitude. Second, let us

take a close look at the numerator of Eq. (31), taking the form $k' \cdot P = \omega' \mathcal{E}(1 - \cos\theta_e)$, where θ_e is the angle between $\mathbf{k}'$ and $\mathbf{v}$. Since $\omega'\mathcal{E}$ and the denominator are of the same order of magnitude, it is clear that $\Xi_1 \ll 1$ is obtained only at $\theta_e \ll 1$, when $k' \cdot P(t) \approx \frac{1}{2}\omega' \mathcal{E}\theta_e^2$. Therefore, in intuitive terms, Eq. (31) requires that the angle between the emitted photon wave vector $\mathbf{k}'$ and the time-dependent velocity associated with the particle classical motion should be much smaller than 1 for all times. In fact, even in the case when emission takes place at a certain time t (when the radiation formation length is short with respect to the characteristic size of the electron trajectory), the phase of emission [see Eq. (32)] is determined by a time integral up to the emission time t.

We can reformulate Eqs. (31) and (33) in terms of the laser and electron parameters. It may be accomplished as follows. We start by evaluating the transverse oscillations of the particle velocity around its average direction, determined by the initial momentum $\mathbf{p}$. According to Eq. (6), the amplitude of the momentum oscillations, induced by the electric field, is $m\xi$, so that $P_\perp \lesssim m\xi$. In addition, the average longitudinal momentum is $P_\parallel \sim m\gamma$. Consequently, one may obtain a crude estimation for the maximal value of the angle θ_e. Namely, the particle's trajectory lies within a cone with angle $\sim P_\perp/P_\parallel \sim \xi/\gamma$. Since, as established above, the emission angle is $\sim 1/\gamma$, the wave vector of the emitted photon $\mathbf{k}'$ is restricted by a cone whose angle is $(1+\xi)/\gamma$. Therefore, $\theta_e \lesssim (1+\xi)/\gamma$ and one may deduce that $\Xi_1 \approx O([1+\xi]/\gamma)^2$. On the other hand, the relative deviation of the energy is $\Xi_2 \approx O(|\mathcal{E} - \mathcal{E}_{av}|/\mathcal{E}_{av}) \approx O(\xi/\gamma)$. As a result, the required conditions given by Eqs. (31) and (33) are reduced to

$$\gamma \gg 1 + \xi. \tag{34}$$

This revised applicability criterion for the semiclassical method is manifestly more restrictive as compared to the original one ($\gamma \gg 1$) claimed by Baier and Katkov in [39,40].

This discrepancy calls for an explanation. Reviewing the Baier-Katkov derivation suggests that the approximations given by Eqs. (31) and (33) were utilized by them as well (see Eqs. (2.23– 2.25) in [40]). Hence, the arising question is: How could they obtain a relaxed validity condition? Their argument may be presented as follows. For ultrarelativistic particles, the main contribution to the emission originates from the part of the trajectory where $\theta_e < 1/\gamma$. Hence, an approximation for the transition amplitude that holds only in the vicinity of the formation length is sufficient. By definition, on the radiation formation region $\theta_e < 1/\gamma$ so that $\Xi_1 \ll 1$ is satisfied. If, in addition, one may assume that the formation length is short enough so that $\mathcal{E}$ may be regarded as constant, then both Eqs. (31) and (33) are fulfilled on the region where the radiation is formed. We argue, however, that even though the main contribution originates from this part of the trajectory, Eqs. (31) and (33) should hold on the entire cycle. In order to see why, let us take a close look at Eq. (14), describing the transition amplitude. Suppose the formation time for a certain emitted photon is centered in the vicinity of t_*. Due to the periodicity, the integrand of (14) in $t_* + T$ would be identical except for an additional phase $e^{i\psi_{np}T}$. Hence, the transition amplitude contains a series of sequential and equal contributions which interfere with each other generating the harmonic structure. In order to reproduce the correct phase between these contributions, the approximation should be valid through the entire cycle and not only on the emission regions since ψ at the emission time t contains integration over time up to the emission moment. Alternatively, one may instantly infer it from the fact that the energy conservation given by Eq. (18), determining the harmonic structure, involves the mean value of the incoming and outgoing particles energies $\mathcal{E}_{av}, \mathcal{E}'_{av}$, averaged on the entire cycle. To conclude the discussion, if the interference of radiation from consecutive cycles of the field, which generates the harmonic structure of the spectrum, is neglected, then the Baier-Katkov approach is valid for the ultrarelativistic condition $\gamma \gg 1$. However, the applicability condition for the accurate description of the harmonic structure of the emission spectrum is given by Eq. (34) derived above.

IV. CIRCULAR MOTION

Let us calculate the intensity emitted by an electron in a REF with vanishing initial momentum ($\mathbf{p} = 0$) corresponding to a circular classical trajectory. This initial condition is chosen for the following reasons. First, the simple classical motion allows for analytical expressions. Second, in this case $\gamma = \xi \gg 1$, so that the original Baier-Katkov condition is fulfilled, but our new restrictive one discussed above, i.e., Eq. (34), is not. In this way, our argument could be put to a test. Third, a circular trajectory corresponds as well to an electron interacting with PWF in the case of a certain initial momentum choice (see the Appendix). As a consequence, we may compare the emission predicted by full quantum calculations for two different EM configurations sharing the same classical trajectory.

In the following, we further elaborate the results obtained in Sec. II, i.e., Eqs. (17), (18), and (23), assuming $\mathbf{p} = 0$. First, one may notice that owing to the azimuthal symmetry, the transition amplitude does not depend on the angle φ so it can be integrated out. Accordingly, from now on, the photon is assumed to be emitted in the x-z plane, without loss of generality. Moreover, one may see that due to the δ function in Eq. (24), I_s depends on a single degree of freedom. Hence, it may be represented as a function of either θ or ω'. In the first case, the solution of the integral in Eq. (24) yields

$$\frac{dI_s}{d(\cos\theta)} = \alpha\omega_s'^3 \left|\frac{d\Omega_s}{d\omega'}\right|^{-1}_{\omega'=\omega'_s} \sum_\epsilon |\mathcal{M}_s|^2, \tag{35}$$

where ω'_s are the solution of Eq. (18) for a given θ. In the latter case, the only modification to Eq. (35) is the replacement of the derivative $d\Omega_s/d\omega'$ with $d\Omega_s/d(\cos\theta)$, namely,

$$\frac{dI_s}{d\omega'} = \alpha\omega'^3 \left|\frac{d\Omega_s}{d(\cos\theta)}\right|^{-1}_{\theta=\theta_s} \sum_\epsilon |\mathcal{M}_s|^2, \tag{36}$$

where θ_s are the solutions of Eq. (18) for a given ω'. In principle, the final expressions given by Eqs. (35) and (36) apply for the SC case as well, with the corresponding modification $\Omega_s, \mathcal{M}_s \to \widetilde{\Omega}_s, \widetilde{\mathcal{M}}_s$. In the following sections, the quantities are explicitly calculated. It is explicitly demonstrated, however, that for a circular motion, the SC model yields an angle-independent $\widetilde{\Omega}_s$. As a result, the corresponding function $dI/d\omega'$ takes the form of a series of δ functions, and Eq. (36)

is meaningless. For this reason, we will focus on the angular distribution given in Eq. (35). The only use of Eq. (36) will be in calculating the spectral width of the WKB harmonics, as presented in Sec. V.

A. Harmonics energies

1. SC approach

The first step to be taken in the framework of the SC approach is to obtain the classical trajectory of the incoming particle. For the REF, the classical equation of motion admits an analytical solution, i.e., Eq. (6). The corresponding trajectory $x_\mu = \int v_\mu dt$ may be cast in terms of elliptical integrals. For a vanishing incoming momentum, Eq. (6) is reduced to

$$P_\mu = m[\sqrt{1+\xi^2}, \xi\cos(\omega t), \xi\sin(\omega t), 0]. \tag{37}$$

Consequently, the trajectory takes the simple form

$$\mathbf{x}(t) = \frac{\xi}{\omega\sqrt{1+\xi^2}}[\sin(\omega t)\hat{x} - \cos(\omega t)\hat{y}]. \tag{38}$$

Plugging Eq. (38) into Eq. (27) and keeping in mind that the emitted photon wave vector lies in the x-z plane, one may find the phase $\widetilde{\psi}$,

$$\widetilde{\psi} = \left(\frac{\omega'\mathcal{E}}{\mathcal{E}-\omega'}\right)\left[t - \frac{\xi}{\omega\sqrt{1+\xi^2}}\sin(\omega t)\sin\theta\right]. \tag{39}$$

Since $\mathcal{E} = m\sqrt{1+\xi^2}$ is constant, the nonperiodic part simply reads

$$\widetilde{\psi}_{np} = \frac{\omega'\mathcal{E}}{\omega(\mathcal{E}-\omega')}. \tag{40}$$

Substituting it into the definition given by Eq. (29) of $\widetilde{\Omega}_s$, one finds

$$\widetilde{\Omega}_s = s\omega - \frac{\omega'\mathcal{E}}{\mathcal{E}-\omega'}. \tag{41}$$

Equating $\widetilde{\Omega}_s$ to zero, the relation between the number of absorbed photons and the emitted photon energy is achieved:

$$\widetilde{\omega}'_s = \frac{s\omega\mathcal{E}}{s\omega+\mathcal{E}}. \tag{42}$$

Several insights can be inferred from Eq. (42). Let us consider the low- and high-energy limits. One may see that for $\omega'/\mathcal{E} \ll 1$, we have $\widetilde{\omega}'_s \approx s\omega$. Namely, in the classical limit, the harmonics are simply multiples of the REF frequency, as expected according to the Schott formula [65]. In the high-energy limit, $\widetilde{\omega}'_s$ approaches the initial energy $\mathcal{E}$ for increasing number of absorbed photons, $s \to \infty$. This means that even though the emission probability decays for $\omega' \to \mathcal{E}$, a restriction on s does not exist, giving rise to the emergence of a semicontinuum.

Furthermore, since $\widetilde{\Omega}_s$ appearing in Eq. (41) bears no angular dependence, ω'_s does not depend on θ as well. The meaning is that all the emitted photons associated with a certain harmonics have the same energy. In other words, the harmonics width integrated over the angle, according to the SC formula, is vanishing. It should be noticed that the formula determining the central energy of the PWF harmonics is identical to Eq. (42), as shown in Eq. (A7) of the Appendix. However, as opposed to the SC case, the PWF harmonics do have significant width, as discussed in detail in Sec. V.

2. WKB approach

The harmonics energies ω'_s arise from the solution of the energy-conservation equation (18). Hence, one should obtain $\mathcal{E}'_{av}$, appearing in this equation. For vanishing initial momentum, Eq. (11) reduces to $\mathcal{E}' = \sqrt{m^2 + [e\mathbf{A}(t) + \mathbf{k}']^2}$. Substituting Eq. (3) and writing $\mathbf{k}'$ explicitly, one arrives at

$$\mathcal{E}' = \sqrt{m^2 + (m\xi\cos(\omega t) + \omega'\sin\theta)^2 + \omega'^2\cos^2\theta}. \tag{43}$$

Averaging it over a single cycle, one obtains (see also [61])

$$\mathcal{E}'_{av} = \frac{2}{\pi}\sqrt{G}E_2(\mu), \tag{44}$$

where $E_2(\mu)$ is the complete elliptical integral of the second kind, $\mu \equiv 4m\xi\omega'|\sin\theta|/G$, and the definition

$$G \equiv \omega'^2 + m^2(1+\xi^2) + 2\omega' m\xi|\sin\theta| \tag{45}$$

is introduced. Accordingly, the derivative of Ω_s, appearing in Eq. (35), may be evaluated analytically. Finally, employing $\mathcal{E}, \mathcal{E}'_{av}$, Eq. (18) should be solved numerically for ω'_s.

Even though an analytical expression for ω'_s is not available, several conclusions can be drawn from Eqs. (18) and (44) for Ω_s. Considering the low-energy limit $\omega'/\mathcal{E} \ll 1$, we have $\mathcal{E} \approx \mathcal{E}'_{av}$ so that $\Omega_s \approx \widetilde{\Omega}_s \approx s\omega - \omega'$. Namely, the classical result is recovered. On the other hand, the high-energy spectrum exhibits qualitatively different behavior as compared to the SC result, derived in the previous section. The quantum model predicts a cutoff for the number of absorbed photons, whereas according to the SC approach, s tends, in principle, to infinity. A crude estimation to this cutoff may be obtained as follows. The high-energy tail of the spectrum corresponds to $\omega' \to \mathcal{E}$. Consequently, ω' and $\mathcal{E}$ cancel out in Eq. (18) and it approximately reduces to $s_c\omega \approx \mathcal{E}'_{av}$. In this limit, $\theta \to \pi/2$ so that $\mu \to 1$ and, therefore, $\mathcal{E}'_{av} = 4m\xi E_2(1)/\pi$. Since $E_2(1) = 1$, the cutoff may be estimated as

$$s_c \approx \frac{4m\xi}{\pi\omega}. \tag{46}$$

The dimensionless parameter s_c determines the maximal number of absorbed photons for the REF configuration.

As opposed to the SC approximation, Ω_s bears angular dependence (through $\mathcal{E}'_{av}$). Therefore, various θ values yield different ω'_s, giving rise to a spectral width. In the case examined numerically below, however, it is explicitly shown that the width after angle integration is much smaller as compared to the spacing between neighboring harmonics, so that they may be regarded as discrete as well.

B. Matrix-element calculation

1. SC approach

In order to calculate the matrix element, one must first obtain the periodic part of the phase, $\widetilde{\psi}_p$. From Eq. (39), one may deduce

$$\widetilde{\psi}_p = \frac{s\xi}{\sqrt{1+\xi^2}}\sin\theta\sin(\omega t) \equiv z\sin(\omega t), \tag{47}$$

where ω' was replaced by the harmonic energy $\widetilde{\omega}'_s$ given by Eq. (42), and the following quantity is introduced:

$$z \equiv \frac{s\xi \sin\theta}{\sqrt{1+\xi^2}}. \tag{48}$$

Employing $\widetilde{\psi}_p$ and the momentum P_μ given by Eq. (37), the matrix element Eq. (28) takes the form

$$\widetilde{\mathcal{M}}_s = \epsilon_\mu \widetilde{\mathcal{M}}^\mu_s, \tag{49}$$

where

$$\widetilde{\mathcal{M}}^\mu_s \equiv \frac{m}{\sqrt{\mathcal{E}(\mathcal{E}-\widetilde{\omega}'_s)\widetilde{\omega}'_s}}(B\sqrt{1+\xi^2}, \xi B_1, \xi B_2, 0). \tag{50}$$

The coefficients B, B_1, B_2 are defined as

$$B \equiv \frac{1}{2\pi}\int_0^{2\pi} d\phi e^{i(z\sin\phi - s\phi)}, \tag{51}$$

$$B_1 \equiv \frac{1}{2\pi}\int_0^{2\pi} d\phi \cos\phi e^{i(z\sin\phi - s\phi)}, \tag{52}$$

and

$$B_2 \equiv \frac{1}{2\pi}\int_0^{2\pi} d\phi \sin\phi e^{i(z\sin\phi - s\phi)}, \tag{53}$$

where $\phi = \omega t$. Recalling the integral definition of the Bessel function J_s, one may write

$$B = J_s(z), \quad B_1 = \frac{s}{z}J_s(z), \quad B_2 = -iJ'_s(z). \tag{54}$$

Due to the Ward identity [62], the sum over the photon polarizations is given by

$$\sum_\epsilon |\widetilde{\mathcal{M}}_s|^2 = -\widetilde{\mathcal{M}}^\mu_s \widetilde{\mathcal{M}}_{s,\mu}. \tag{55}$$

Employing Eqs. (49)–(54), we obtain

$$\sum_\epsilon |\widetilde{\mathcal{M}}_s|^2 = K\left\{\xi^2\left[\left(\frac{s^2}{z^2}-1\right)+J'^2_s(z)\right]-J^2_s(z)\right\}, \tag{56}$$

where the following quantity is introduced:

$$K \equiv \frac{m^2}{\mathcal{E}(\mathcal{E}-\widetilde{\omega}'_s)\widetilde{\omega}'_s}. \tag{57}$$

The final result is very similar to the matrix element corresponding to a circularly polarized plane wave, as obtained by Ritus and Nikishov [15] (see the Appendix). The main difference lies within the definition of z.

Since we are interested in the $\xi \gg 1$ domain, the integrals appearing in Eqs. (51)–(53) are rapidly oscillating and therefore may be approximated using the saddle-point technique [15], yielding

$$J_s(z) \approx \left(\frac{2}{s}\right)^{1/3}\mathrm{Ai}(y), \quad J'_s(z) \approx \left(\frac{2}{s}\right)^{2/3}\mathrm{Ai}'(y), \tag{58}$$

where $\mathrm{Ai}(y)$ designates the Airy function, with the argument

$$y \equiv \left(\frac{s}{2}\right)^{2/3}\left(1-\frac{z^2}{s^2}\right). \tag{59}$$

As a result, the sum over polarizations of the squared matrix element reads

$$\sum_\epsilon |\widetilde{\mathcal{M}}_s|^2 \approx K\left\{-\mathrm{Ai}^2(y)+\xi^2\left(\frac{2}{s}\right)^{4/3}[y\mathrm{Ai}^2(y)+\mathrm{Ai}'^2(y)]\right\}. \tag{60}$$

2. WKB approach

In the following, the relation between the quantum and SC matrix elements is established. The WKB matrix element was defined in Eq. (17). Since $\mathcal{E}$ is constant, the periodic part of the phase given by Eq. (15) takes the form

$$\psi_p = \mathcal{E}'_{av}t - \int_{-\infty}^{t} dt'\mathcal{E}'. \tag{61}$$

For the case considered in this work, i.e., $\gamma \approx \xi \gg 1$, the argument ψ is rapidly oscillating and the contribution to the integral comes from the region where $\theta_e < 1/\gamma$, as explained in Sec. III. Therefore, one may use the Baier-Katkov approximation for the phase

$$\psi = \omega'_s t + \int_{-\infty}^{t} dt'(\mathcal{E}'-\mathcal{E}) \approx \frac{\mathcal{E}}{\mathcal{E}-\omega'_s}(k'_s\cdot x), \tag{62}$$

where $k'_s = \omega'_s(1, \sin\theta, 0, \cos\theta)$ is the wave vector of the emitted photon corresponding to the s harmonic, and ω'_s is found according to the procedure described in Sec. IV A 2. Plugging $\int_\infty^t dt'\mathcal{E}'$ from Eq. (62) into Eq. (61) and using $s\omega + \mathcal{E} = \omega'_s + \mathcal{E}'_{av}$, one obtains

$$\begin{aligned}\psi_p &= \mathcal{E}'_{av}t - \mathcal{E}t - \frac{\mathcal{E}}{\mathcal{E}-\omega'_s}(k'_s\cdot x) + \omega'_s t \\ &= s\omega t - \frac{\mathcal{E}}{\mathcal{E}-\omega'_s}(k'_s\cdot x).\end{aligned} \tag{63}$$

Hence, in the vicinity of the saddle point, we have

$$\psi_p - s\omega t \approx -\frac{\mathcal{E}}{\mathcal{E}-\omega'_s}(k'_s\cdot x). \tag{64}$$

Writing explicitly the right wing, we have

$$\psi_p - s\omega t \approx \frac{\mathcal{E}}{\mathcal{E}-\omega'_s}\mathbf{k}'_s\cdot\mathbf{x}_p - s_{\mathrm{eff}}\omega t, \tag{65}$$

where s_{eff}, defined by

$$s_{\mathrm{eff}}\omega \equiv \frac{\omega'_s\mathcal{E}}{\mathcal{E}-\omega'_s}, \tag{66}$$

is an effective (and not necessarily integer) index for which the emitted energy of the SC model coincides with the WKB harmonic ω'_s. One may explicitly verify that even though the functions on the right and left wings of Eq. (65) are not identical, their Taylor expansion up to third order in the vicinity of the saddle point is identical. Additionally, it should be noted that as opposed to $\mathcal{E}-\omega'$ appearing in the denominator of Eq. (28), Eq. (17) contains instead the time-dependent quantity $\mathcal{E}'$. However, Taylor expanding $\mathcal{E}'$ in the vicinity of the saddle point $t = 0$, one observes that the zeroth-order term is $\mathcal{E}-\omega'$ and the first-order one vanishes. Hence, as both the prefactor and the phase of the WKB and SC are identical up

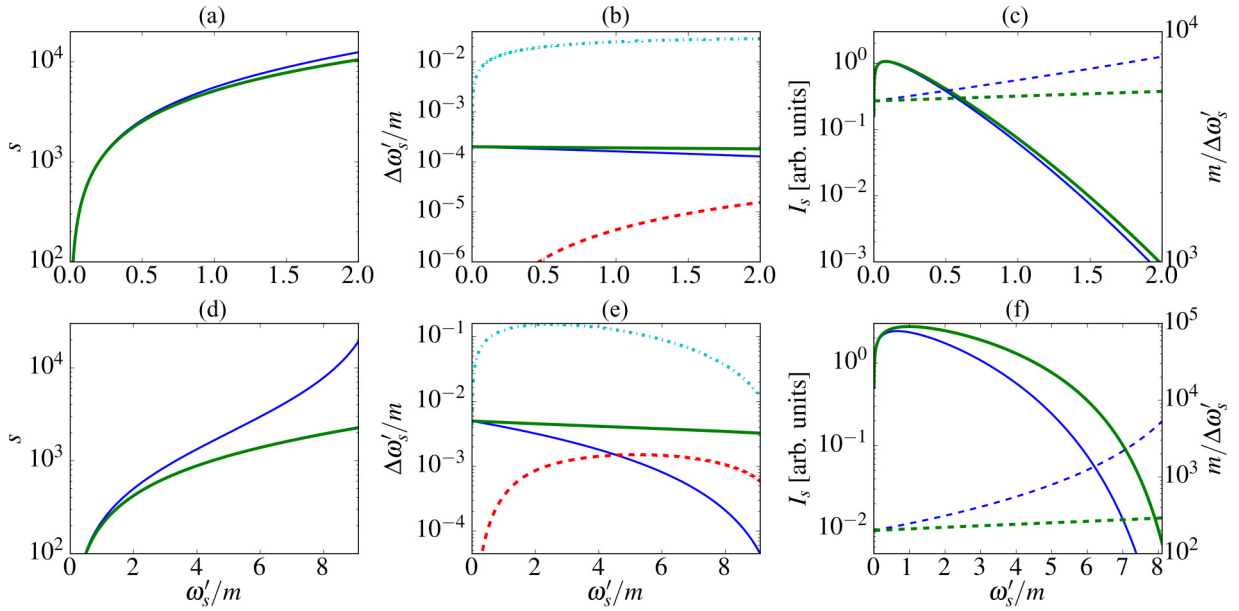

FIG. 2. (a) The number of absorbed photons s vs the emitted photon energy ω'_s: WKB (green line) and SC (blue thin line). The PWF and SC curves coincide. (b) The spectral width of harmonics: WKB (red dashed line) and PWF (turquoise dash-dotted line) (the SC width is vanishing). The gap between neighboring harmonics: WKB (green line) and SC/PWF (blue thin line). (c) The total harmonics intensity (solid line) and the harmonic density (dashed line): WKB (green line) and SC/PWF (blue thin line). The laser parameters are $\xi = 10$, $\omega = 100$ eV, corresponding to $\chi = 0.02$, $I_L = 10^{24}$ W/cm^2. The electron initial momentum is $\mathbf{p} = 0$. (d)–(f) Similar to (a)–(c), but with $\omega = 2.55$ keV, corresponding to $\chi = 0.5$, $I_L = 10^{27}$ W/cm^2.

to the required order near the saddle point, one may write

$$\mathcal{M}_s \approx \widetilde{\mathcal{M}}_{s_{\rm eff}}. \tag{67}$$

Namely, the WKB matrix element coincides with the SC one corresponding to an effective harmonic index $s_{\rm eff}$, for which the emitted energy ω' would be the same. Alternatively, Eq. (67) may be expressed in terms of $\mathcal{T}_{if}$. Comparing Eq. (14) and Eq. (17), one may observe that

$$\mathcal{M}_s = \frac{1}{T}\mathcal{T}_{0T}(k'_s), \tag{68}$$

where the subscript $0T$ stands for the integration limits designated as t_i, t_f in Eq. (14). As a result, Eq. (67) may be written as

$$\mathcal{T}_{0T}(k') \approx \widetilde{\mathcal{T}}_{0T}(k'). \tag{69}$$

Intuitively, this result may be explained as follows. As discussed in Sec. III, the difference between $\mathcal{T}, \widetilde{\mathcal{T}}$ originates from the interference between different cycles. The matrix-element integration, however, is limited to a single cycle and a single saddle point contributing to the emission. Accordingly, the amplitudes of the two methods are sampling of the same function, where the difference arises from the different sampling frequency, namely, the harmonics $\omega'_s, \widetilde{\omega}'_s$, respectively.

V. NUMERICAL RESULTS

In the following, the emission properties are calculated numerically via the quantum WKB and SC methods for the REF configuration, as well as compared with the well-known PWF result. The nonlinear parameter is $\xi = 10$ and the electron initial momentum is $\mathbf{p} = 0$. Two cases were considered, corresponding to different values of the quantum parameter $\chi = \xi^2(\omega/m)$. The higher χ, the larger the discrepancy between WKB and SC. The case of $\chi = 0.5$, presented in Figs. 2(d)–2(f), illustrates the expected effect in the spectral distribution. It may be realized with $\omega = 2.55$ keV, corresponding to an x-ray free-electron laser (XFEL) with an intensity of about $I_L \approx 10^{27}$ W/cm^2. A smaller but still visible effect can be obtained, as shown in Figs. 2(a)–2(c), even by using less demanding conditions, $\omega = 100$ eV, $\chi = 0.02$, and the laser intensity $I_L \approx 10^{24}$ W/cm^2. These intensities lay above the presently available ones [4,5,66]. Nevertheless, improvements of the focusing technique to approach the diffraction limit may allow for such intensities in the future [67].

A. Harmonic structure

Figures 2(a) and 2(d) show the relation between the number of absorbed laser photons s and the emitted photon energy ω'_s for the lower and higher intensity, respectively. The values for the WKB model stem from the numerical solution of Eq. (18), as explained in Sec. IV A 2. The SC and PWF predictions are analytical and identical, as may be seen in Eqs. (42) and (A7). For small values of the emitted photon energy, both SC and WKB curves reduce to the classical prediction. The deviation occurs near the high-energy tail of the spectrum. For the lower intensity shown in Fig. 2(a), it amounts to about 20% for harmonics still having a significant intensity; see Fig. 2(c). For the high-intensity case depicted in Fig. 2(d), the discrepancy is of orders of magnitude and the different asymptotic behavior for $\omega' \to \mathcal{E}$ is manifested. One may see that according to the SC model, the harmonic number s asymptotically increases, while the WKB model

predicts a finite cutoff. The cutoff value is $s_c \approx 2550$, in agreement with the theoretical estimation of Eq. (46). The physical meaning is that in a REF, a higher amount of energy would be depleted from the external field as compared to the same emission in a PWF. Furthermore, since the difference between the absorbed laser energy $s\omega$ and the emitted photon energy ω' is converted to the kinetic energy of the electron, it implies that for the PWF, the emission is accompanied by higher outgoing electron energy.

The gap between harmonics $\Delta\omega'_s$ for the various approaches, as well as the spectral width of the WKB and PWF harmonics, are shown in Figs. 2(b) and 2(e). The width is defined so that 2/3 of the total intensity is contained within its boundaries and is calculated using Eq. (36). Notice that the SC harmonics have no width, as shown analytically in Sec. IV A 1. First, one may observe that the gap changes only slightly for the WKB, but decreases significantly for the SC (40 and 1.4 times for the high and low intensity, respectively). Second, the WKB harmonics width is significantly lower than the gap, implying that they may be regarded as discrete. The PWF width, however, is always much higher than the gap, so that the spectrum is continuous and the harmonics cannot be distinguished. Thus, the quantum mechanical calculation of emission corresponding to two distinct field configurations yields different results, even though the associated classical trajectories are similar. Therefore, we can conclude that the classical trajectory does not solely determine the emission, but rather the particular features, such as the dispersion relation of the wave vector, of the driving EM field play a role as well.

The total spectral intensity of the harmonics, obtained by integrating over the angle θ [see Eq. (35)], is presented in Figs. 2(c) and 2(f). The PWF and SC curves coincide, as in Figs. 2(a) and 2(d). One can see that the high-energy WKB harmonics are stronger than the SC ones (40 and 1.4 times for the high and low intensity, respectively). The relation between the discrepancies depicted in these figures and those appearing in Figs. 2(a) and 2(d) call for a clarification. As we demonstrate both analytically and numerically in the next section, the harmonic-averaged spectrum takes the same shape for all models, to an excellent approximation. Hence, the concentration of harmonics obtained by the SC/PWF models near the high-energy tail of the spectrum implies that their intensity should be lower, as indeed is the case. In order to further illustrate this point, this figure shows the normalized harmonics density $m/\Delta\omega'_s$ as well. The latter indicates clearly that for the SC, the harmonics density is much higher. In other words, the WKB exhibits distant and intense harmonics, while the SC predicts weak and spectrally dense ones.

B. Average spectrum

Figure 3 presents the harmonic-averaged spectrum (i.e., the harmonics power divided by $\Delta\omega'_s$) of the WKB and SC models, as well as the PWF and LCFA spectrum. Let us provide a physical explanation for this result. One may see that all curves coincide to a very good approximation. From the relation given by Eq. (69) between $\mathcal{T}_{0T}, \widetilde{\mathcal{T}}_{0T}$, it follows that for a single-cycle pulse, the quantum and SC methods should yield approximately the same transition amplitude, and hence the same spectrum. In the following, we argue that the

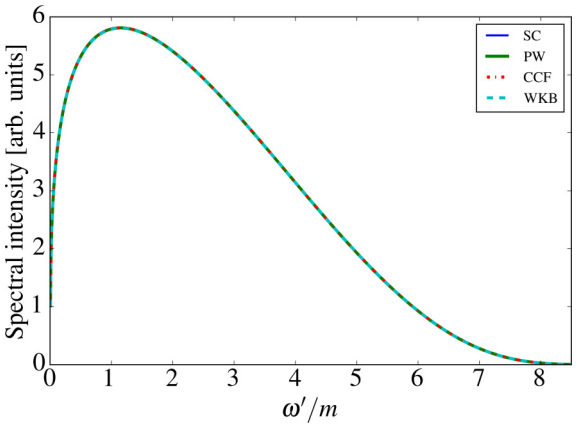

FIG. 3. The harmonics-averaged spectrum: SC (blue thin line), PWF (green line), and WKB (turquoise dashed line) as compared to the LCFA expression (red dash-dotted line). The laser parameters are $\xi = 10$, $\omega = 2.55$ keV, corresponding to $\chi = 0.5$, $I_L = 10^{27}$ W/cm^2. The electron initial momentum is $\mathbf{p} = 0$. All curves coincide to a very good approximation.

transition from a single cycle to a periodic pulse gives rise to the concentration of the emitted energy in discrete harmonics (which are different for the two models as seen above) without changing the harmonic-averaged spectrum.

One may notice that $\mathcal{T}_{if}$ given by Eq. (14) may be cast in the form

$$\mathcal{T}_{if} = \int_{-\infty}^{\infty} dt\, f(t,\omega') e^{i\omega' t}, \tag{70}$$

where the quantity $f(t,\omega')$ is defined as

$$f(t,\omega') \equiv \frac{(\epsilon\cdot P)}{\sqrt{\omega'\mathcal{E}\mathcal{E}'}} \exp\left[\left(\int_{\infty}^{t} dt'\mathcal{E}' - \int_{-\infty}^{t} dt'\mathcal{E}\right)\right]. \tag{71}$$

It resembles a Fourier transform except for the fact that $f(t,\omega')$ depends on ω' as well as on t. Furthermore, according to the derivation given in Secs. II and III [see Eq. (24)], the intensity is proportional to

$$\frac{dI}{d\cos\theta} \propto \int_{-\infty}^{\infty} \omega'^3 |\mathcal{T}_{if}|^2 d\omega', \tag{72}$$

which takes the same form as the energy integration over a Fourier spectrum, except for the ω'^3 factor. In order to take advantage of this analogy, we recall one of the Fourier transform features.

Let us consider a function $q(l)$ which is nonvanishing only in the interval $0 < l < L$. Its Fourier transform reads

$$Q(v) \equiv \int_{-\infty}^{\infty} q(l) e^{-ivl} dl = \int_{0}^{L} q(l) e^{-ivl} dl. \tag{73}$$

Now we use $q(l)$ to define a periodic function,

$$q_p(l) \equiv q(l - nL), \quad n \equiv \left\lfloor \frac{l}{L} \right\rfloor, \tag{74}$$

where $\lfloor\rfloor$ designates the flooring function. Owing to its periodicity, the new function may be written as a Fourier

series,

$$q_p(l) = \sum_j \frac{Q(v_j)}{L} e^{ilv_j}, \quad v_j = \frac{2\pi j}{L}. \tag{75}$$

Accordingly, its Fourier transform reads

$$Q_p(v) = \frac{2\pi}{L} \sum_j \delta(v - v_j) Q(v_j). \tag{76}$$

Namely, the transition from a single to periodic function induced "roaming" of the spectral energy to discrete frequencies (harmonics) without changing the average energy. In order to observe it explicitly, let us consider the energy contained in the interval $v_j < v < v_{j+1}$,

$$\int_{v_j}^{v_{j+1}} dv |Q_p(v)|^2 = \frac{1}{2}[Q^2(v_j) + Q^2(v_{j+1})][v_{j+1} - v_j], \tag{77}$$

where the definition of v_j as well as the identity $\delta^2(v - v_j) = (L/2\pi)\delta(v - v_j)$ were employed. One may see that Eq. (77) approximately equals the integral over a single-cycle spectrum $\int_{v_j}^{v_{j+1}} dv |Q(v)|^2$, given that the envelope function $Q(v)$ changes only slightly in the interval under consideration.

The same reasoning applies in our case, given that the functions ω'^3 and $f(t, \omega')$ are slowly varying envelope functions which stay almost constant on the frequency scale of the above-mentioned "energy roaming," i.e., $\omega' \to \omega' + \Delta\omega'_s$. Since $\Delta\omega'_s \leqslant \omega$, as demonstrated in Figs. 2(b) and 2(e), and as $\xi \gg 1$ corresponds to $\omega' \gg \omega$, this condition is satisfied and hence one should expect the harmonic-averaged spectrum to be equivalent to the single-cycle one. The same argument applies for the SC case, so that its harmonic-averaged spectrum recovers the single-cycle one. Finally, since the WKB and SC single-cycle spectrum is equivalent, as established above, one may deduce that the harmonic-averaged spectra of the WKB and SC approaches coincide as well.

Having established the agreement of the harmonic-averaged spectrum with the LCFA formula, we call attention to the following points. First, even though all scenarios asymptotically approach the LCFA limit, one may expect certain deviations for finite ξ values, even in the strong-field regime. The nature of deviations, however, is substantially different for the two configurations. The PWF spectrum, as was shown in [44–46], is continuous for the most part and the discrepancies are to be found mainly for the first few harmonics, as their formation time is comparable to the field cycle. For the REF calculation, however, the deviations are much more manifest (i.e., the harmonics are discrete) and are not limited to the low-energy tail but are rather present through the entire spectrum.

Second, the phenomenon illustrated in this section, namely, the reduction of a rich harmonic structure to the plain universal LCFA form after averaging, is not unique. It also appears in the well-established problem of radiation in constant magnetic field [20], where the exact quantum harmonics may be replaced by the synchrotron formula (which is identical to the LCFA one). Whether or not approximating of the spectrum by its harmonic-averaged one is justified depends on the required resolution. In the quantum regime, the energy of the emitted photon is of the order of magnitude of the emitting electron. In order to resolve the harmonics structure, however, a measurement resolution of the order of magnitude of ω (the oscillation frequency) is required. For the case of synchrotron facilities, for instance, the electron energy is well above GeV, while the typical frequency lies below the MHz domain. Since these two energy scales are separated by so many orders of magnitude, considering the harmonics structure is meaningless. In the case considered in our manuscript, on the other hand, the number of harmonics amounts to several thousand, so that the emitted photon energy is about 3–4 orders of magnitude above the field frequency. It implies that accuracy of about 0.1 percent is required. This is indeed beyond present-day capability, but may be accessible in the future.

VI. DISCUSSION AND CONCLUSIONS

In this paper, the radiation emitted by a particle in the presence of REF, which may represent either a plasma wave or the antinode of a standing wave, has been explored. An analytical emission rate has been derived within the Furry framework, employing the WKB approximation for the dressed particle wave function.

This expression has been utilized as a benchmark to the SC method. A detailed comparison has been carried out, showing that the SC result is valid if the conditions given by Eqs. (31) and (33) are met. These requirements may be formulated intuitively as follows. First, the angle between the emitted photon and the particle classical velocity should be much smaller than 1 for all times. Second, the particle energy should be approximately constant in time. We further demonstrate that these conditions may be approximated by a simple criterion given by Eq. (34). Namely, the γ factor should dominate over the nonlinearity parameter ξ. Careful examination of the SC derivation suggests that these approximations were employed by Baier and Katkov as well. Nevertheless, they claimed that their approximation holds given that the particle is ultrarelativistic, which is far less restrictive than Eq. (34). Their reasoning is that ultrarelativistic velocity assures that Eqs. (31) and (33) are satisfied on the radiation formation length. We show, on the other hand, that the phase difference between the emission amplitudes from subsequent cycles is accrued during the whole electron motion within the laser period and outside of the formation length, and, therefore, for its correct description the mentioned approximations should be fulfilled for all times of interaction. Only in this case can the harmonic structure of the spectrum be correctly reproduced.

In order to explicitly demonstrate that the validity condition is Eq. (34) rather than $\gamma \gg 1$ and to explore the nature of deviations, a particular initial momentum ($\mathbf{p} = 0$) has been chosen, corresponding to $\gamma = \xi$. Qualitative deviations in the harmonic structure were demonstrated. The harmonic-averaged spectra, on the other hand, were shown to be approximately equivalent. An analytical explanation of the latter result has been given in Sec. V B, relying on the relation given by Eq. (69) between the transition amplitudes calculated by the two methods.

Furthermore, we took advantage of an additional feature of the particular case studied in detail above, namely, the fact that the classical trajectory associated with the incoming

electron is a circular motion. An identical classical trajectory corresponds to an electron counterpropagating a plane wave, given that its initial momentum is appropriately tuned [see (A1) in the Appendix]. It allows for a comparison between two quantum calculations of different EM configurations, i.e., PWF and REF, sharing the same initial classical dynamics. The following differences were found:

(i) *Width*. The PWF harmonics width has been shown to be much larger than their spacing. Accordingly, the spectrum is continuous and coincides with the LCFA result. The REF on the other hand, yields discrete harmonics.

(ii) *The harmonic structure*. High-energy photon emission involves an increasing number of absorbed laser photons in the PWF case, while for the REF a cutoff s_c emerges, limiting the possible number of absorbed photons.

The following insights may be inferred from these discrepancies. First, they serve as evidence that two distinct EM fields corresponding to the same classical trajectory may give rise to different emission characteristics. In the realm of the quantum calculation, this finding poses no problem. For each EM field, the energy-momentum conservation takes a different form and thus yields dissimilar outgoing momentum for a given emitted photon. Consequently, the wave functions associated with the outgoing particle are not identical, giving rise to various spectra. On the other hand, this result explicitly contradicts the main paradigm of the SC approach, stating that a certain incoming particle trajectory corresponds to a distinct emission, regardless of the EM field. This implies that an additional assumption, presumably related to the scattering process kinematics, is incorporated in the SC expression. The examination of the SC derivation suggests that this assumption is not related to the approximations given by Eqs. (31) and (33) discussed above. This conclusion stems from the fact that even prior to the introduction of these approximations, the emission expression depends exclusively on the incoming particle classical dynamics [i.e., $P_\mu(t)$]; see, for instance, Eq. (2.22) in [40]. Since in the case of REF we have coincidence of the SC result with WKB (discussed in Sec. III) without this obscure approximation, one may reckon that it is automatically satisfied for the particular case of the REF. Further investigation is requested in order to discover this assumption and shed light on the exact criterion which predicts for which conditions the classical trajectory does not solely determine the emission.

Second, we recall that according to the Nikishov-Ritus hypothesis given by Eq. (1), the spectrum should depend on a single parameter χ and take the form of the LCFA expression. Hence, the fact that the REF spectrum is discrete is remarkable. Moreover, the spectrum is characterized by the additional dimensionless quantity s_c, which is absent in the PWF spectrum. On the other hand, the REF harmonic-averaged spectrum coincides with the LCFA one. Thus, our results demonstrate that Eq. (1) is sufficient only for the harmonic-averaged spectrum to be approximated by the LCFA formula, whereas the exact one may still feature the harmonics structure.

Third, the cutoff s_c predicted in this paper for the REF may have another implication. It has been recently suggested that significant depletion of the laser field due to hard photons emission may lead to the breakdown of the external field approximation, which is the cornerstone of the Furry strong-field QED picture [68,69]. This scenario is of special interest for the QED cascades calculations, as it involves high particle density corresponding to substantial field depletion. The threshold corresponding to this breakdown has been established [68] using the scaling $s \sim \xi^3$ for the number of absorbed laser photons associated with a typical emission process. Consequently, our result $s_c \propto m\xi/\omega$, which scales differently with the field parameters, should lead to an altered breakdown condition. This issue will be addressed in a separate paper. Fourth, the REF is shown in this paper to be a quantum system exhibiting discrete emission modes in the x-/γ-ray regimes. Such a property may be appealing from the prospective of development of future novel radiation sources.

ACKNOWLEDGMENTS

The authors are grateful to Antonino Di Piazza for helpful discussions. E.R. acknowledges financial support from the Alexander von Humboldt Foundation.

APPENDIX: PLANE-WAVE AND CONSTANT CROSSED FIELD FORMULAS

First, let us obtain the initial momentum for a particle counterpropagating a plane wave which results in a circular motion, similar to the REF case. We recall that in this case, the time-dependent momentum is given by [15]

$$P_\mu = p_\mu - eA^l_\mu + \frac{e^2a^2}{2(k^l\cdot p)}k^l_\mu, \tag{A1}$$

where the vector potential A^l takes the same form as Eq. (3) with k replaced by $k^l=(\omega,0,0,\omega)$. As a result, for initial momentum $(p_0,0,0,p_z)$ satisfying $p_z = e^2a^2/[2(p_0-p_z)]$, the z component of the momentum vanishes, leading to the same classical trajectory (circle) and quantum parameter χ as in the REF problem we consider.

The intensity of the radiation emitted by a scalar particle interacting with a circularly polarized plane wave is given by [15]

$$\frac{dI}{du} = \alpha m^2\frac{u}{(1+u)^3}\sum_s\left\{-J_s^2(z)+\xi^2\left[\left(\frac{s^2}{z^2}-1\right)J_s^2(z) + J_s'^2(z)\right]\right\}, \tag{A2}$$

where the relation between u and the emitted photon energy for ultrarelativistic particles reads

$$u = \frac{\omega'}{\mathcal{E}-\omega'}, \tag{A3}$$

so that $\omega' = u\mathcal{E}/(1+u)$. The Bessel function argument is given by

$$z \equiv \frac{\xi^2\sqrt{1+\xi^2}}{\chi}\sqrt{u(u_s-u)}. \tag{A4}$$

Each harmonic is nonvanishing on the interval $0<u<u_s$ where

$$u_s \equiv \frac{2s\chi}{\xi(1+\xi^2)}. \tag{A5}$$

The harmonic spectral location is defined according to the peak emission, corresponding to $u = u_s/2$. Using Eq. (A3), one may write it in terms of the emitted photon energy,

$$\omega_s' = \frac{u_s}{2(1+u_s/2)}\mathcal{E}. \tag{A6}$$

Employing Eq. (A5) as well as $\chi = \xi\mathcal{E}\omega/m^2$ and $\mathcal{E} = m\sqrt{1+\xi^2}$, one obtains

$$\omega_s' = \frac{s\omega\mathcal{E}}{s\omega+\mathcal{E}}. \tag{A7}$$

Notice that this expression is identical to the one obtained for the SC model.

The LCFA expression arises from Eq. (A2) by using the saddle-point analysis (similar to the derivation in the SC matrix-element section) and replacing the discrete harmonics with a continuous variable, namely,

$$\frac{dI}{du} = \frac{\alpha m^2 u}{2(1+u)^3}\left(\frac{u}{2\chi}\right)^{1/3}\int_{-\infty}^{\infty} d\tau \times\left[-\mathrm{Ai}^2(y)+\left(\frac{2\chi}{u}\right)^{2/3}[y\mathrm{Ai}^2(y)+\mathrm{Ai}'^2(y)]\right], \tag{A8}$$

where

$$y \equiv \left(\frac{u}{2\chi}\right)^{2/3}[1+\tau^2]. \tag{A9}$$

[1] The Gemini laser: https://www.clf.stfc.ac.uk/Pages/Laser-system-Gemini.aspx (unpublished).
[2] The Extreme Light Infrustructure (ELI): https://eli-laser.eu/ (unpublished).
[3] The XCELS project: http://www.xcels.iapras.ru (unpublished).
[4] The LCLS project: https://lcls.slac.stanford.edu/ (unpublished).
[5] The XFEL project: http://www.xfel.eu (unpublished).
[6] T. Tajima and G. Mourou, Phys. Rev. ST Accel. Beams **5**, 031301 (2002).
[7] J. T. Mendonça and S. Eliezer, in *Applications of Laser-Plasma Interaction*, edited by S. Eliezer and K. Mima (CRC, Boca Raton, FL, 2009).
[8] E. Esarey, C. B. Schroeder, and W. P. Leemans, Rev. Mod. Phys. **81**, 1229 (2009).
[9] A. Macchi, M. Borghesi, and M. Passoni, Rev. Mod. Phys. **85**, 751 (2013).
[10] J. Schwinger, Phys. Rev. **82**, 664 (1951).
[11] T. N. Wistisen, A. Di Piazza, H. V. Knudsen, and U. I. Uggerhøj, Nat. Commun. **9**, 795 (2018).
[12] J. M. Cole, K. T. Behm, E. Gerstmayr, T. G. Blackburn, J. C. Wood, C. D. Baird, M. J. Duff, C. Harvey, A. Ilderton, A. S. Joglekar, K. Krushelnick, S. Kuschel, M. Marklund, P. McKenna, C. D. Murphy, K. Poder, C. P. Ridgers, G. M. Samarin, G. Sarri, D. R. Symes, A. G. R. Thomas, J. Warwick, M. Zepf, Z. Najmudin, and S. P. D. Mangles, Phys. Rev. X **8**, 011020 (2018).
[13] K. Poder, M. Tamburini, G. Sarri, A. Di Piazza, S. Kuschel, C. D. Baird, K. Behm, S. Bohlen, J. M. Cole, D. J. Corvan, M. Duff, E. Gerstmayr, C. H. Keitel, K. Krushelnick, S. P. D. Mangles, P. McKenna, C. D. Murphy, Z. Najmudin, C. P. Ridgers, G. M. Samarin, D. R. Symes, A. G. R. Thomas, J. Warwick, and M. Zepf, Phys. Rev. X **8**, 031004 (2018).
[14] A. Di Piazza, C. Müller, K. Z. Hatsagortsyan, and C. H. Keitel, Rev. Mod. Phys. **84**, 1177 (2012).
[15] V. I. Ritus, J. Sov. Laser Res. **6**, 497 (1985).
[16] W. H. Furry, Phys. Rev. **81**, 115 (1951).
[17] D. M. Volkov, Z. Phys. **94**, 250 (1935).
[18] A. I. Nikishov, Sov. Phys. JETP **32**, 690 (1971).
[19] N. P. Klepikov, Zh. Esp. Teor. Fiz **26**, 19 (1954).
[20] A. A. Sokolov and I. M. Ternov, *Radiation from Relativistic Electrons* (American Institute of Physics, New York, 1986).
[21] P. J. Redmond, J. Math. Phys. **6**, 1163 (1965).
[22] V. B. Berestetskii, E. M. Lifshitz, and L. P. Pitaevskii, *Quantum Electrodynamics*, Course in Theoretical Physics, Vol. 4 (Pergamon, Oxford, 1982).
[23] A. I. Nikishov and V. I. Ritus, Sov. Phys. JETP **19**, 529 (1964).
[24] T. O. Müller and C. Müller, Phys. Rev. A **86**, 022109 (2012).
[25] A. Di Piazza, E. Lötstedt, A. I. Milstein, and C. H. Keitel, Phys. Rev. A **81**, 062122 (2010).
[26] P. Panek, J. Z. Kamiński, and F. Ehlotzky, Phys. Rev. A **65**, 022712 (2002).
[27] P. Panek, J. Z. Kamiński, and F. Ehlotzky, Phys. Rev. A **69**, 013404 (2004).
[28] E. Lötstedt and U. D. Jentschura, Phys. Rev. A **80**, 053419 (2009).
[29] F. Mackenroth and A. Di Piazza, Phys. Rev. A **83**, 032106 (2011).
[30] T. Heinzl, D. Seipt, and B. Kämpfer, Phys. Rev. A **81**, 022125 (2010).
[31] A. Ilderton, Phys. Rev. Lett. **106**, 020404 (2011).
[32] M. Boca and V. Florescu, Phys. Rev. A **80**, 053403 (2009).
[33] A. I. Titov, B. Kampfer, A. Hosaka, and H. Takabe, Phys. Part. Nucl. **47**, 456 (2016).
[34] A. R. Bell and J. G. Kirk, Phys. Rev. Lett. **101**, 200403 (2008).
[35] J. G. Kirk, A. R. Bell, and I. Arka, Plasma Phys. Control. Fusion **51**, 085008 (2009).
[36] I. V. Sokolov, N. M. Naumova, J. A. Nees, and G. A. Mourou, Phys. Rev. Lett. **105**, 195005 (2010).
[37] A. M. Fedotov, N. B. Narozhny, G. Mourou, and G. Korn, Phys. Rev. Lett. **105**, 080402 (2010).
[38] R. Duclous, J. G. Kirk, and A. R. Bell, Plasma Phys. Control. Fusion **53**, 015009 (2011).
[39] V. N. Baier and V. M. Katkov, Sov. Phys. JETP **26**, 854 (1968).
[40] V. N. Baier, V. M. Katkov, and V. M. Strakhovenko, *Electromagnetic Processes at High Energies in Oriented Single Crystals* (World Scientific, London, 1998).
[41] E. N. Nerush, I. Yu. Kostyukov, A. M. Fedotov, N. B. Narozhny, N. V. Elkina, and H. Ruhl, Phys. Rev. Lett. **106**, 035001 (2011).
[42] N. V. Elkina, A. M. Fedotov, I. Yu. Kostyukov, M. V. Legkov, N. B. Narozhny, E. N. Nerush, and H. Ruhl, Phys. Rev. ST Accel. Beams **14**, 054401 (2011).
[43] T. Grismayer, M. Vranic, J. L. Martins, R. A. Fonseca, and L. O. Silva, Phys. Plasmas **23**, 056706 (2016).

[44] A. Di Piazza, M. Tamburini, S. Meuren, and C. H. Keitel, Phys. Rev. A **98**, 012134 (2018).
[45] A. Di Piazza, M. Tamburini, S. Meuren, and C. H. Keitel, Phys. Rev. A **99**, 022125 (2019).
[46] I. Ilderton, B. King, and D. Seipt, Phys. Rev. A **99**, 042121 (2019).
[47] A. Di Piazza, Phys. Rev. Lett. **113**, 040402 (2014).
[48] A. Di Piazza, Phys. Rev. A **91**, 042118 (2015).
[49] A. Di Piazza, Phys. Rev. Lett. **117**, 213201 (2016).
[50] A. Di Piazza, Phys. Rev. A **95**, 032121 (2017).
[51] A. Gonoskov, A. Bashinov, I. Gonoskov, C. Harvey, A. Ilderton, A. Kim, M. Marklund, G. Mourou, and A. Sergeev, Phys. Rev. Lett. **113**, 014801 (2014).
[52] E. Raicher and S. Eliezer, Phys. Rev. A **88**, 022113 (2013).
[53] E. Raicher, S. Eliezer, and A. Zigler, Phys. Lett. B **750**, 76 (2015).
[54] W. Becker, Physica A **87**, 601 (1977).
[55] C. Cronstrom and M. Noga, Phys. Lett. A **60**, 137 (1977).
[56] S. Varro, Laser Phys. Lett. **10**, 095301 (2013).
[57] T. Heinzl, A. Ilderton, and B. King, Phys. Rev. D **94**, 065039 (2016).
[58] E. Raicher, S. Eliezer, and A. Zigler, Phys. Rev. A. **94**, 062105 (2016).
[59] F. Mackenroth, N. Kumar, N. Neitz, and C. H. Keitel, Phys. Rev. E **99**, 033205 (2019).
[60] E. Brezin and C. Izykson, Phys. Rev. D **2**, 1191 (1970).
[61] G. R. Mocken, M. Ruf, C. Müller, and C. H. Keitel, Phys. Rev. A **81**, 022122 (2010).
[62] M. E. Peskin and D. V. Schroeder, *An Introduction to Quantum Field Theory* (Perseus Books, Reading, 1995).
[63] T. N. Wistisen and A. Di Piazza, Phys. Rev. A **98**, 022131 (2018).
[64] T. N. Wistisen and A. Di Piazza, arXiv:1904.02997v1.
[65] G. A. Schott, *Electromagnetic Radiation* (Cambridge University Press, Cambridge, 1912).
[66] M. Fuchs *et al.* Nat. Phys. **11**, 964 (2015).
[67] A. Ringwald, in *Proceeding of Erice, Workshop On Electromagnetic Probes Of Fundamental Physics*, edited by W. Marciano and S. White (World Scientific, River Edge, 2003).
[68] D. Seipt, T. Heinzl, M. Marklund, and S. S. Bulanov, Phys. Rev. Lett. **118**, 154803 (2017).
[69] A. Ilderton and D. Seipt, Phys. Rev. D **97**, 016007 (2018).